An Ultrasensitive 14GHz 1.12mW EPR Spectrometer in 28nm CMOS

Luya Zhang, Ali M. Niknejad
EECS, University of California, Berkeley, CA, USA
luyazhang@berkeley.edu

***Abstract* — This work presents an integrated sensing platform for clinical electron paramagnetic resonance (EPR) spectroscopy. The sensor core comprises a LC tank whose resonance frequency matches the radical Larmor frequency and detects its EPR signal via the change of the tank inductance. To achieve high sensitivity, the inductance variation is measured in a self-mixing interferometric fashion with an on-off modulated RF source to attenuate the noise from the source and the readout circuitry. A sensor prototype was fabricated in 28 nm CMOS. It achieved a spin sensitivity of 6.1×10^8 spins/rtHz with only 1.12 mW power consumption, demonstrating over 10x improvement in both power and sensitivity compared with prior arts of similar system complexity.**

***Keywords* — paramagnetic resonance, microwave resonators, magnetic sensors, biomedical transducers, interferometry.**

I. Introduction

Electron paramagnetic resonance (EPR) is a spectroscopic technique that detects the interaction between unpaired electrons of a radical and microwave radiation in the presence of a dc magnetic field. It has been established as the most powerful technique for studying free radicals and other paramagnetic species, such as reactive oxygen species and transition metal ions, in the biological systems. For instance, it can provide non-invasive and accurate assessment of local oxygen levels in the surgical wounds, signaling the healing status which helps optimize the treatment plan. Sharing similar detection principles with magnetic resonance imaging (MRI), EPR offers several orders of magnitude higher sensitivity by operating at a much higher frequency. Despite these advantages, EPR is predominantly used in the scientific laboratories and has not yet advanced to the clinical practices. One major obstacle is associated with the existing EPR instrumentation, which is bulky, expensive and extremely complicated to operate, and thereby restricts its deployment in various clinical settings, such as point-of-care or body implants.

With the rapid development of (Bi)CMOS technologies, several integrated EPR spectrometers have been demonstrated [1]–[3]. In [1], an RF transceiver was implemented to detect the absorption of microwave energy by EPR. However, it consumes 2W of power, which causes significant heating and undesired interference with the radical EPR responses. On the other hand, oscillator-based EPR spectrometers [2], [3] were reported with a better energy efficiency. In the latter case, it detects the change of radical magnetic permeability caused by EPR, which is manifested as the change of the oscillation frequency. The sensitivity, however, is affected by the temperature drift and transistor flicker noise, which also change the oscillation frequency.

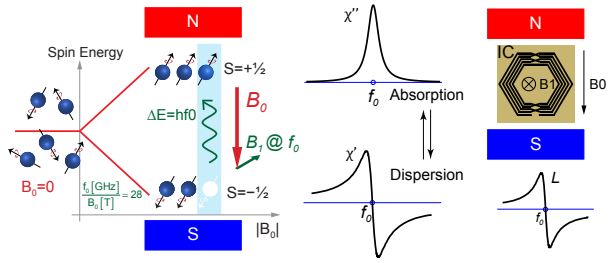

Fig. 1. Principle of EPR spectroscopy and the equivalence of absorption EPR spectrum and dispersion EPR spectrum. The latter allows EPR to be measured as the change of the inductance.

A clinically useful EPR spectroscopy demands both high sensitivity and high energy efficiency. To meet these goals, this work proposes a new sensing topology to simultaneously improve the detection limit and power efficiency. To minimize the transducer noise contribution, a passive LC resonator is employed to measure the EPR induced magnetic permeability change. An RF source is capacitively injected to the resonator to excite EPR, and to enforce a near-quadrature phase relation with the EPR signal. A self-mixing interferometric phase detection is then performed to extract the EPR signal as well as to cancel out the noise from the RF source. As a validation, a 14 GHz EPR spectrometer prototype was fabricated in the 28 nm CMOS process, which achieves 6.1×10^8 spins/rtHz sensitivity with only 1.12 mW power consumption, over $10\times$ better than the existing single-chip EPR spectrometers.

II. EPR Sensor Design

A. Sensing Principle

Fig. 1 illustrates the principle of EPR spectroscopy. With the exertion of a dc magnetic field B_0, the energy level of unpaired electrons within the radical will split apart. If a second ac magnetic field B_1 is applied with a proper orientation (perpendicular to B_0), the electron spin will be excited to the upper energy level by absorbing a photon from B_1, which produces the EPR absorption spectrum around the Larmor frequency f_0 (f_0/B_0 =28 GHz/T). According to Kramers-Kronig relations, this absorption signal is always accompanied with a dispersion signal, which is manifested as the real part of radical ac magnetic susceptibility. Therefore, the EPR spectrum of a radical can be obtained by measuring the inductance variation of a sensing coil positioned in contact with the radical.

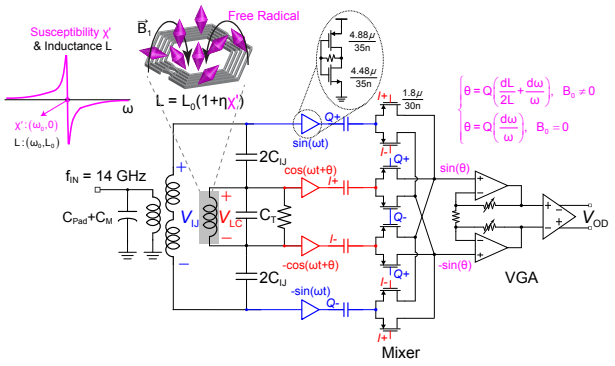

Fig. 2. System block diagram.

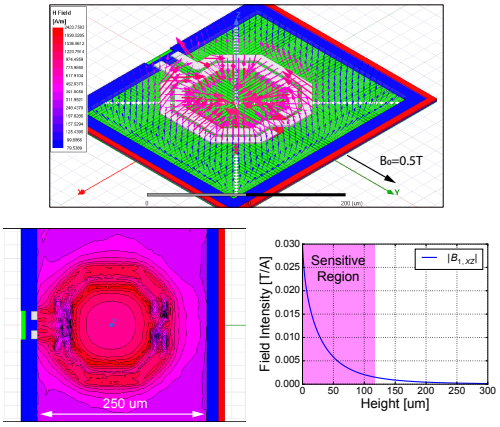

Fig. 3. HFSS simulation results of the 3-dimensional B_1 fields created by the sensing coil (top), and the distribution of B_{1x}, B_{1z} components (bottom), which illustrates the effective sensitivity volume.

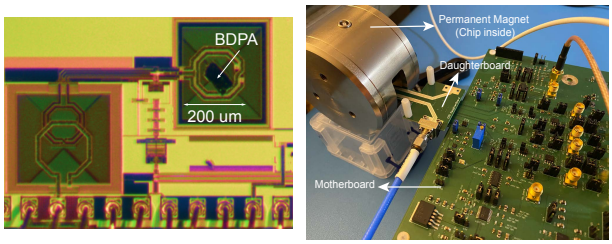

Fig. 4. Chip micrograph with a BDPA sample deposited in the center of the sensing inductor (left) and measurement setup (right).

B. System Implementation

To measure the change of inductance around f_0 (14 GHz in this work) with a high sensitivity, a capacitively coupled LC tank is utilized as the sensing frontend, which is shown in Fig. 2. The tank capacitor C_{T} and the injection capacitor C_{IJ} in parallel resonate with the sensing inductor L at f_0, which forces a quadrature relation between the tank output V_{LC} and the injection input V_{IJ}. At $f = f_0 + \delta f$, the relation between V_{LC} and V_{IJ} around f_0 can be derived as

$$\begin{aligned} \left\| \frac{V_{\mathrm{LC}}}{V_{\mathrm{IJ}}} \right\| &= Q \frac{C_{\mathrm{IJ}}}{C_{\mathrm{T}}} \\ \angle \frac{V_{\mathrm{LC}}}{V_{\mathrm{IJ}}} &= Q\left(\frac{\delta f}{f_0} + \frac{\delta L}{2L_0}\right) + \frac{\pi}{2} \end{aligned} \tag{1}$$

where $\delta L = L_0 \cdot \chi'$ and χ' is the radical ac magnetic susceptibility. As the frequency of V_{IJ} is swept in the vicinity of f_0, the relative phase difference between V_{LC} and V_{IJ} deviates from 90° by a quantity that is proportional to both δL and δf, multiplied by a gain-boosting factor equal to the tank qualify factor Q ($Q = 20.8$). Because the inductance only changes in the presence of B_0, two measurements with $B_0 = 0$ T and $B_0 = 0.5$ T are sufficient to extract the EPR signal χ'. To extend the sensing volume, L should be maximized without sacrificing the tuning range. Moreover, according to (1), the ratio between C_{IJ} and C_{T} should be selected to equalize the relative amplitude between V_{IJ} and V_{LC}, so that the propagation delays of the subsequent mixer drivers are matched to avoid introducing extra phase error. In this work, $L = 1$ nH and $C_{\mathrm{T}}/C_{\mathrm{IJ}} = 19$. A double-balanced voltage-commutative passive mixer is employed to convert the aforementioned phase signal into voltage, which is then amplified by a VGA and fed to an external ADC.

Compared with oscillator-based inductor sensing solutions [2]–[5], the proposed method eliminates the noisy transistors, thereby exhibiting a much better sensitivity and immunity against the temperature and supply variations. In addition, self-mixing based phase detection [6] is performed, which not only brings a free transducer gain of Q before any amplifier stages, but also cancel out the phase noise from the injection source. In addition, since the signal is down-converted to dc, the offset and flicker noise from the mixer and VGA are of great concern. To avoid SNR degradation, system-level chopping is applied by pulse-modulating the 14 GHz injection signal at 50 kHz to shift the signal frequency above the flicker corner. The residual noise is solely the thermal noise of the coil and mixer/VGA, which can be attenuated by averaging.

In addition to noise, another critical factor that affects SNR is the orientation of B_0. Since EPR demands that B_1 be perpendicular to B_0, while the B_1 fields created by a planar inductor extend to all directions, as depicted in Fig. 3, a filling factor η is introduced ($\delta L = L_0 \cdot \eta\chi'$, $\eta < 1$) to account for the signal loss. EM simulations were used to identify the optimal B_0 direction that maximizes η. It was found that when B_0 orients along the inductor feeds (the y axis in Fig.3), η reaches $\eta_{\max} = 0.32$. Moreover, the effective sensing volume can be estimated from the distribution of B_{1x} and B_{1z}, as plot in Fig. 3, which is approximately 7.5 nL.

III. Measurement Results

A sensor prototype was fabricated in the 28 nm CMOS process. Fig. 4 gives the chip micrograph and the experimental setup. For optimal power and linearity performance, the supply voltage of the RF and BB sections are set to 0.6 V and 1.2 V, respectively. The entire chip consumes 1.12 mW. A compact 0.5 T permanent magnet ($80\times80\times55$ mm^3) was used to provide a uniform B_0 field. The chip was positioned inside the magnet and oriented properly according to the above description. A 50 kHz pulse-modulated injection signal

Table 1. Comparison with the state-of-the-art integrated EPR spectrometers.

	This Work	ISSCC'18 [3]	ISSCC'16 [2]	TMTT'15 [1]	JMR'12 [4]	Rev. Sci.'08 [5]
Field Strength B_0 [T]	**0.5**	0.5	0.5	0.15	0.96	0.35
Operation Frequency [GHz]	**11.2-14.5**	11.8-14.2	13.2-14.3	3.8-4.8	27	9
Spin Sensitivity [spins/rtHz]	**6.1×10^8**	8×10^9	4×10^9	Not specified	2×10^8	1×10^{10}
Sensitivity Volume [nL]	**7.5**	15/channel*	27	10000**	1	1
ASIC Power [mW]	**1.12**	15/channel*	15	2000	75	160
Technology	**28 nm CMOS**	130 nm CMOS	130 nm CMOS	130 nm BiCMOS	130 nm CMOS	350 nm CMOS
EPR Spectrum	**Dispersion**	Dispersion	Dispersion	Absorption	Dispersion	Dispersion
Tolerance to PVT Variations	**High**	Low	Low	High	Low	Low
System Size and Complexity	**Low**	Low	Low	Low	High	High

* Eight channels in total.
** Used an off-chip resonator on the PCB.

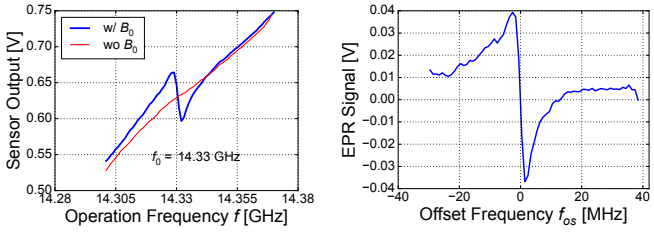

Fig. 5. Measured EPR spectrum of a BDPA crystal.

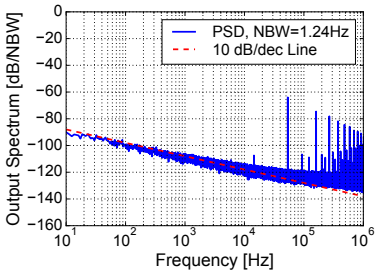

Fig. 6. Measured output power spectrum density (PSD), with a system-level chopping at 50 kHz.

was generated off-chip and coupled to the sensor through a wide-band on-chip transformer.

An *in-vitro* bio-experiment was performed using crystalline BDPA, an organic radical. BDPA was deposited at the center of the sensing inductor prior to the experiment. To characterize its EPR properties, two measurements with and without the permanent magnet were conducted. The EPR spectrum of BDPA can be extracted by taking the difference between the two measurements. The results are summarized in Fig. 5.

To examine the sensor sensitivity level, its output power spectrum density (PSD) was measured, as shown in Fig. 6. For noise analysis, the PSD is elevated by 3 dB due to the subtraction operation when obtaining the EPR spectrum. The noise density around the signal frequency (50 kHz) is about 0.71 μV/rtHz. Following the method given by [4], with a BDPA sample of known size ($110\times40\times5$ μm^3) and known spin density (1.57×10^{27} spins/m^3), the sensor can achieve a spin sensitivity of 6.1×10^8 spins/rtHz.

IV. Conclusion

The key performance metrics of the sensor are summarized in Table 1, and compared with the state-of-the-art integrated EPR spectrometers. It demonstrates the best energy efficiency and almost the highest spin sensitivity. Although a slightly better sensitivity was shown in [4], it consumed much more power and required an AM modulation of the B_0 field, which substantially increases the system complexity and cost. The sensor sensitivity volume can be further enlarged by duplicating the sensing coil into an array. Overall, offering a high sensitivity and power efficiency, this work paves the way for EPR to be translated into routine clinical practice.

Acknowledgment

The authors would like acknowledge the TSMC University Shuttle Program for chip fabrication and Integrand EMX for electromagnetic simulators.

References

[1] X. Yang and A. Babakhani, "A single-chip electron paramagnetic resonance transceiver in 0.13-μm SiGe BiCMOS," *IEEE Transactions on Microwave Theory and Techniques*, vol. 63, no. 11, pp. 3727–3735, Nov. 2015.

[2] J. Handwerker, B. Schlecker, U. Wachter, P. Radermacher, M. Ortmanns, and J. Anders, "28.2 A 14GHz battery-operated point-of-care ESR spectrometer based on a 0.13μm CMOS ASIC," in *2016 IEEE International Solid-State Circuits Conference (ISSCC)*, Jan. 2016, pp. 476–477.

[3] A. Chu, B. Schlecker, K. Lips, M. Ortmanns, and J. Anders, "An 8-channel 13GHz ESR-on-a-Chip injection-locked VCO-array achieving 200μM-concentration sensitivity," in *2018 IEEE International Solid - State Circuits Conference - (ISSCC)*, Feb. 2018, pp. 354–356.

[4] J. Anders, A. Angerhofer, and G. Boero, "K-band single-chip electron spin resonance detector," *Journal of Magnetic Resonance*, vol. 217, pp. 19–26, Apr. 2012.

[5] T. Yalcin and G. Boero, "Single-chip detector for electron spin resonance spectroscopy," *Review of Scientific Instruments*, vol. 79, no. 9, p. 094105, Sep. 2008.

[6] L. Zhang and A. M. Niknejad, "Design and analysis of a microwave-optical dual modality biomolecular sensing platform," *IEEE Journal of Solid-State Circuits*, vol. 55, no. 3, pp. 639–649, Mar. 2020.